Precise Interference Analysis of OFDMA Time-Asynchronous Wireless Ad-hoc Networks

Khairi Ashour Hamdi, *Senior Member, IEEE*

***Abstract*—This paper presents a unified mathematical performance analysis of the physical layer in orthogonal frequency division multiple access (OFDMA) wireless ad hoc networks, where several independent transmitter-receiver pairs share a common wideband channel in a local area environment. Multiuser interference (MUI) occurs when the signals from different users arrive at a given receiver with arbitrary timing misalignments, leading to the destruction of the orthogonality between subcarriers. Precise interference analysis in white Gaussian noise and Rayleigh multipath fading is developed in a partially loaded OFDMA network. New exact expressions of symbol and bit error rates are given in the case of interleaved subcarrier assignment schemes. On the other hand, tight upper bounds and accurate improved Gaussian approximations are developed for arbitrary subcarrier assignment schemes. Furthermore, expressions of the cutoff rates are derived and employed to estimate the spectral efficiency in bits/sec./Hz. These are used to quantify the improvement in the spectral efficiency that can be achieved by a common MUI mitigating technique based on the extension of guard intervals and dynamic positioning of FFT windows.**

***Index Terms*—Ad-hoc networks, multiaccess communication, orthogonal frequency-division multiplexing (OFDM).**

I. Introduction

ORTHOGONAL Frequency Division Multiple Access (OFDMA) is a promising wireless access technique [1]-[3] which has recently been employed in several new networking technologies such as WiMAX [4] and DVB-RCT [5].

In OFDMA, the total system bandwidth is partitioned into a set of orthogonal subcarriers which are assigned to multiple users for simultaneous transmissions. OFDMA is sensitive and vulnerable to timing errors which destroy the orthogonality and result in multiuser interference (MUI). To maintain orthogonality among sub-carriers, the signals from all active users must arrive at the receiver synchronously. Several multiuser synchronization techniques have been proposed in cellular-based OFDMA networks which guarantee that all OFDM signals arriving to the base station are perfectly aligned. However, most of these techniques are based on closed-loop time correction techniques [6] which require the receiver to estimate all arrival times.

On the other hand, each node in the OFDMA ad hoc network can communicate directly with other nodes without a central base station. Therefore, it will be expensive to implement these multiuser synchronization techniques at every receiver of the OFDMA ad hoc network. One particular method for combating the MUI caused by the loss of orthogonality, which suits the ad hoc OFDMA networks, is based on the extension of the cyclic prefix (CP) lengths beyond what is required to control the inter-symbol interference (ISI) caused by the multipath fading [6]. Although CPs of adequate lengths have the desired effect of rendering asynchronous signals to appear orthogonal at the receiver, and thus alleviate the resultant MUI, increasing the length of the guard-interval, however, has its own cost as it will reduce the net transmission rate in the system. It is therefore of both theoretical and practical interests to obtain a better knowledge on the effectiveness of the time-guard intervals in combatting MUI in OFDMA ad hoc networks. Motivated by this problem, the aim of this paper is to develop accurate mathematical analysis of the MUI at the physical layer (PHY) of OFDMA ad hoc networks, which takes into account accurately the effects of the propagation delays and the spatial distribution of users.

Recent performance analysis of ad hoc OFDMA has focused on the media access control (MAC) and the upper layers ignoring the MUI that may occur at the PHY layer due to timing misalignments (e.g. [7]-[10]). On the other hand, performance analysis of single user OFDM in the presence of timing and synchronization errors has received considerable research efforts, and several accurate mathematical methods have been developed for bit and symbol error rate analysis in different channel models (e.g., [11]-[13]). Unfortunately, interference modelling in multiuser OFDM involves a larger number of random variables, and therefore the extension of these methods to the analysis of ad hoc OFDMA is not straightforward.

Relevant research on interference analysis of asynchronous OFDMA include [14]-[19], which have developed accurate interference models for centralized OFDMA networks (where all users communicate with a common base station). The effects of both timing and frequency errors are considered in [14], [15], [19], whereas [16] and [18] focus only on the timing errors. As far as the error rate evaluation is concerned, [14] is based on a brute averaging technique which requires large computational efforts, whereas [15], [17], [18] have opted for Monte-carlo simulation methods. On the other hand, [16] and [19] are limited to the analysis of the average signal to interference-plus-noise ratio (SINR).

In this paper, we develop a new precise interference analysis of OFDMA with arbitrary subcarrier assignment schemes in multipath Rayleigh fading of arbitrary power-delay profiles. This leads to new precise expressions for error and cutoff rates

Manuscript received May 14, 2008; revised November 25, 2008 and June 14, 2009; accepted September 30, 2009. The associate editor coordinating the review of this paper and approving it for publication was S. Blostein.

K. A. Hamdi is with the School of Electrical & Electronic Engineering, The University of Manchester, Sackville Street, Po Box 88, Manchester M60 1QD United Kingdom (e-mail: k.hamdi@manchester.ac.uk).

Digital Object Identifier 10.1109/TWC.2010.01.080255

with interleaved subcarrier assignment schemes. Moreover, new accurate bounds and approximations are developed for systems with arbitrary subcarrier assignment schemes. These results can be used to assess the impact of time-misalignments on the spectral efficiency of OFDMA ad hoc network, and to quantify the potential improvement achievable by the implementation of extended CPs and dynamic positioning of the FFT windows.

This paper is organized as follows. In Section II, we describe the model of the OFDMA under consideration. In Section III, we present accurate interference analysis, and derive closed-form expressions for the distribution of the SINR for interleaved and block subcarrier assignments. These are used to obtain new expressions for the bit and symbol error probabilities in Section IV, and cutoff rates in Section VI. In Section V, we study the impact of FFT window positions on the overall efficiency of OFDMA. Numerical examples are given in Section VII, and Section VIII concludes the paper.

II. The Model

Let $K+1$ transmitter-receiver pairs share a common wideband channel using OFDMA, where each user is assigned one or several subcarriers, and the subcarrier frequencies from all users form a set of N orthogonal carriers. The lowpass equivalent of the signal transmitted by the kth user takes the form

$$s_k(t) = A \sum_{i=-\infty}^{\infty} \sum_{l=0}^{N+N_g-1} B_{k,l}^{[i]} \; p\left(t - lT_s - i\left(T+T_g\right)\right) \quad (1)$$

where A is the amplitude, T is the (useful) OFDM symbol time, and T_g is the CP time interval ($T+T_g$ is the total OFDM block time). $T_s = \frac{T}{N}$ is the sampling period, and $N_g = \frac{T_g}{T_s}$ is the number of CP samples, $p\left(t\right)$ is the transmitter pulse, and $\left\{B_{k,l}^{[i]},\ l = 0, 1, ..., N+N_g-1\right\}$ is the IFFT block transmitted during the ith symboling interval, where

$$B_{k,l}^{[i]} = \frac{1}{\sqrt{N}} \sum_{n \in \mathcal{A}_k} b_{k,n}^{[i]} e^{j\frac{2\pi nl}{N}}, \quad l = 0, 1, ..., N+N_g-1 \quad (2)$$

and $b_{k,n}^{[i]}$ are the complex modulated symbols. In this paper, we assume a square M-QAM modulation with Gray coding, where $\mathrm{Re}\left\{b_{k,n}^{+}\right\}$ and $\mathrm{Im}\left\{b_{k,n}^{+}\right\}$ are selected independently over the set $\left\{\pm 1, \pm 3, ..., \pm\left(\sqrt{M}-1\right)\right\}$ with equal probabilities. Here, $M = 2^2, 2^4, 2^6, 2^8, ...$ is the constellation size.

In (2), $\mathcal{A}_k$ is the set of subcarriers allocated to user k, where $\bigcup_{k=0}^{K} \mathcal{A}_k = \{0, 1, 2, \ldots, N-1\}$, and $\mathcal{A}_k \bigcap \mathcal{A}_j = \emptyset$ for $k \neq j$. As far as how the subcarriers are assigned to different users, two subcarrier assignment schemes are mostly referred in the literature, namely; *a*) *interleaved subcarrier assignment schemes*, where subcarriers of each user are spread over all frequency band, and *b*) *block (or subband) subcarrier assignment schemes*, where each user is assigned a continuous block of subcarriers.

In order to simplify the mathematical analysis, let the reference receiver be at the centre of a circular service area of radius D, and let the desired transmitter be located at distance d_0 from the reference receiver, whereas all other transmitters are uniformly distributed over the circular service area.

We assume a multipath Rayleigh fading channel, where the impulse response of the channel between the kth transmitter and the reference receiver can be represented as follows

$$h_k\left(t\right) = d_k^{-\beta/2} \sum_{c=0}^{C-1} g_{k,c} \delta\left(t - \frac{d_k}{v} - \varepsilon_k - \tau_{k,c}\right) \quad (3)$$

where C is the total number of multipaths, β is the pathloss exponent and d_k is the distance between the kth transmitter and the reference receiver. v is the speed of light, $\tau_{k,0} < \tau_{k,1} < \ldots \tau_{k,C-1} < \tau_{\max}$, and $\tau_{\max}$ is the maximum delay spread of the multipath channel. $g_{k,c}, k = 0, 1, \ldots, K, c = 0, 1, .., C-1$, are independent and identically distributed circular symmetric complex Gaussian RVs of zero mean and variances $\gamma_c = \mathbb{E}\left[\left|g_{k,c}\right|^2\right]\ \forall k$. Without any loss of generality, we normalize the power such that $\sum_{c=0}^{C-1} \gamma_c = 1$.

In (3), ε_k, $k = 0, 1, \ldots, K$ model the time synchronization errors between the different transmitters. In order to simplify the presentation and focus on the impact of the maximum propagation delays and the random users' locations on the overall spectral efficiency, we assume in this paper that $\varepsilon_k = 0\ \forall k$. (That is all transmitters are assumed perfectly synchronized.) The present analysis can be extended straightforwardly to include the effect of nonzero ε_k.

The signal at the receiver is given by the superposition of signals from all active users, and can be represented as shown in (4), where $w\left(t\right)$ is the (filtered) additive complex white Gaussian noise (AWGN) with a variance $\frac{N_0}{T_s}$, and $p'\left(t\right)$ is the combined impulse response of the transmitter and receiver filters. We assume, for the sake of simplicity, that $p'\left(t\right) = 1$ when $t \in \left(0, T_s\right)$ and $p'\left(t\right) = 0$ otherwise.

In (4), α_k takes values in $\{0, 1\}$ and represents the status of the kth user (inactive/active), $k = 1, 2, \ldots, K$. We assume that $\alpha_1, \alpha_2, \ldots, \alpha_K$ are mutually independent, and $\Pr\left\{\alpha_k = 1\right\} = q$, and $\Pr\left\{\alpha_k = 0\right\} = 1 - q\ \forall k$.

Demodulation for a given user is accomplished by first acquiring time and frequency synchronization for that user, sampling at T_s intervals, and then apply the samples into the N-point FFT demodulator. Without any loss of generality, let us consider user 0 as the reference user and let the time instant $\frac{d_0}{v}$ be precisely known at the reference receiver. Then the output samples during the 0th time interval $\left(\frac{d_0}{v}, \frac{d_0}{v} + T + T_g\right)$ are shown in (5), where $\chi_{t,k,c}$ is the sample taken from the cth path of the k signal at sampling instance t. w_t, $t = 0, 1, \ldots, N+N_g-1$, are samples from the AWGN with variance $\frac{N_0}{T_s}$.

The OFDMA demodulator discards the CP samples and performs an N-point FFT on the remaining sequence $\left\{r_{N_g}, r_{N_g+1}, ..., r_{N+N_g-1}\right\}$. The FFT output at subcarrier m (assuming subcarrier $m \in \mathcal{A}_0$) is shown in (6), where the last step is proven in Appendix A. On the other hand, the first term is a standard result for OFDM systems with sufficient CP, e.g. [2, Ch. 2]. Here, $G_{0,m} = \sum_{c=0}^{C-1} g_{0,l} e^{-j2\pi mc/N}$ is the frequency-domain channel gain at subcarrier m, $W_m = \frac{1}{\sqrt{N}} \sum_{t=N_g}^{N+N_g-1} w_t e^{-j2\pi tm/N}$ is the AWGN in the mth subcarrier, which is still a zero-mean complex Gaussian RV with variance $\frac{N_0}{T_s}$. $\left\{b_{k,n}^{-}, b_{k,n}^{+}\right\}$ represent the two consecutive symbols from subcarrier n which occupy the time interval

$$r(t) = A\sum_{k=0}^{K} d_k^{-\beta/2}\alpha_k \sum_{c=0}^{C-1} g_{k,c} \sum_{i=-\infty}^{\infty} \sum_{l=0}^{N+N_g-1} B_{k,l}^{[i]}\; p'\left(t - lT_s - i\left(T+T_g\right) - \tfrac{d_k}{v} - \tau_{k,c}\right) + w(t) \tag{4}$$

$$r_t = Ad_0^{-\beta/2}\sum_{c=0}^{C-1} g_{0,c}\chi_{t,0,c} + A\sum_{k=1}^{K}\alpha_k d_k^{-\beta/2}\sum_{c=0}^{C-1} g_{k,c}\chi_{t,k,c} + w_t, \quad t = 0,1,...N+N_g-1 \tag{5}$$

$$\begin{aligned}
\eta_m &= \tfrac{1}{\sqrt{N}} \sum_{t=N_g}^{N+N_g-1} r_t e^{-j2\pi tm/N} \\
&= Ad_0^{-\beta/2}G_{0,m}b_{0,m}^{[0]} + A\sum_{k=1}^{K}\alpha_k d_k^{-\beta/2}\sum_{c=0}^{C-1} g_{k,c}\left\{\tfrac{1}{\sqrt{N}}\sum_{t=N_g}^{N+N_g-1}\chi_{t,k,c}e^{-j2\pi tm/N}\right\} + W_m \\
&= Ad_0^{-\beta/2}G_{0,m}b_{0,m}^{[0]} + A\sum_{k=1}^{K}\alpha_k d_k^{-\beta/2}\sum_{c=0}^{C-1} g_{k,c}\left\{\sum_{n\in\mathcal{A}_k}\left(b_{k,n}^{-} - b_{k,n}^{+}\right)\mathcal{G}\left(n-m, \tfrac{d_k-d_0}{v}+\tau_{k,c}\right)\right\} + W_m
\end{aligned} \tag{6}$$

$$\mathcal{G}(p,y) = \begin{cases} 0, & 0 < y \bmod (T+T_g) \le T_g \\ \dfrac{\sin\left(\pi \dfrac{\left\lfloor \frac{y \bmod (T+T_g)}{T_s}\right\rfloor - N_g}{N} p\right)}{N\sin\left(\frac{\pi}{N}p\right)} e^{j\frac{\pi p}{N}\left(\left\lfloor \frac{y \bmod (T+T_g)}{T_s}\right\rfloor + N_g - 1\right)}, & T_g < y \bmod (T+T_g) \le T+T_g. \end{cases} \tag{7}$$

$\left(\frac{d_0}{v}, \frac{d_0}{v}+T+T_g\right)$, and the function $\mathcal{G}(p,y)$ is defined as shown in (7).

Equation (6) describes accurately the FFT output when all signals are perfectly synchronized in frequency. The first term represents the contribution of the desired signal, whereas the second term represents the MUI arising from the time misalignments of all multipath components. It is worth mentioning that if the receiver was not perfectly synchronized with the desired transmitter, then additional multiple access interference (MAI) component would also appear in (6), e.g., [19].

It is worth noticing that the term $\left(b_{k,n}^{-} - b_{k,n}^{+}\right)\mathcal{G}\left(m-n, \frac{d_k-d_0}{v}+\tau_{k,c}\right)$ in (6), which represents the MUI contribution of the cth path of subcarrier n, vanishes whenever either $b_{k,n}^{-} = b_{k,n}^{+}$ or $\left(\frac{d_k-d_0}{v}+\tau_{k,c}\right) \bmod (T+T_g) < T_g$. That is, the orthogonality between subcarriers m and n (when allocated to different users) is maintained whenever $b_{k,n}^{-} = b_{k,n}^{+}$ regardless of the level of the time offset between them. On the other hand, when $b_{k,n}^{-} \neq b_{k,n}^{+}$, then the orthogonality is preserved only if the time offset falls within the CP time-interval.

The decision variables (assuming perfect channel state estimation) are given by $\mathrm{Re}\left\{\frac{\eta_m}{G_{0,m}}\right\}$ and $\mathrm{Im}\left\{\frac{\eta_m}{G_{0,m}}\right\}$ $\forall m \in \mathcal{A}_0$. As far as the statistics of the decision variables $\frac{\eta_m}{G_{0,m}}$ is concerned, notice from (6) that since W_m and $g_{k,c}\forall k,c$ are independent complex Gaussian RVs, then $\frac{\eta_m}{G_{0,m}}$ becomes a "conditionally" complex Gaussian RV. The conditional variance is shown in (8).

It is worth mentioning that in arriving at this conclusion (that the decision variables are conditionally Gaussian), we have not introduced any kind of the commonly used approximations (e.g. standard or improved Gaussian approximations, which are used in interference analysis of wireless communication systems). Hence, the known standard closed-form expressions of the bit or symbol error rates in AWGN channels can be used to obtain exact closed-form expressions for the "conditional probability of errors" which depend solely on the SINR, with the value of SINR shown in (9), where $\rho_k = \frac{d_k}{D}$ and $\Delta = \frac{D}{v}$ is the maximum propagation delay. On the other hand, $E_s = D^{-\beta}A^2T_s$ is the (peak) received symbol energy when the useful transmitter is located at the boundary of the service area (i.e. when $d_0 = D$).

Note that SINR in (9) is a mixture of a ratio of RVs. This is in contrast to the classical interference analysis which is based on the standard Gaussian approximation (SGA), where the accumulated mutliple-access interference is approximated by a pure Gaussian noise having a deterministic variance, and therefore the denominator of the SINR is not a RV.

The evaluation of average bit or symbol error rates reduces therefore into the computation of averages of the form $\mathbb{E}\left[\mathrm{erfc}\sqrt{\mathrm{SINR}}\right]$. Towards this end, we derive in the next section expressions for the probability distribution function of SINR.

III. SINR Statistics

In this section we derive exact expressions for the cumulative distribution function (CDF) of SINR, $\Pr\left(\mathrm{SINR} \le z\right)$. Notice at first that the numerator of (9), $|G_{0,m}|^2$, is an ex-

$$\mathrm{Var}\left(\eta_m | G_{0,m}, d_k, \alpha_k, b_{k,n}^-, b_{k,n}^+ \forall k,n\right) = \frac{1}{|G_{0,m}|^2}\left\{A^2 \sum_{k=1}^{K} d_k^{-\beta}\alpha_k \sum_{c=0}^{C-1}\gamma_c \left|\sum_{n\in\mathcal{A}_k}\left(b_{k,n}^- - b_{k,n}^+\right)\mathcal{G}\left(n-m, \tfrac{d_k-d_0}{v}+\tau_{k,c}\right)\right|^2 + \tfrac{N_0}{T_s}\right\}. \quad (8)$$

$$\mathrm{SINR} = \frac{|G_{0,m}|^2}{\sum_{k=1}^{K}\left(\frac{\rho_k}{\rho_0}\right)^{-\beta}\alpha_k \sum_{c=0}^{C-1}\gamma_c\left|\sum_{n\in\mathcal{A}_k}\left(b_{k,n}^- - b_{k,n}^+\right)\mathcal{G}(n-m,(\rho_k-\rho_0)\Delta+\tau_{k,c})\right|^2 + \frac{\rho_0^\beta}{E_s/N_0}} \quad (9)$$

$$\Pr\left(\mathrm{SINR}\le z | \alpha_k, \rho_k, b_{k,n}^-, b_{k,n}^+ \forall k,n\right) = 1 - e^{-z\left(\sum_{k=1}^{K}\left(\frac{\rho_k}{\rho_0}\right)^{-\beta}\alpha_k \sum_{c=0}^{C-1}\gamma_c\left|\sum_{n\in\mathcal{A}_k}\left(b_{k,n}^- - b_{k,n}^+\right)\mathcal{G}(n-m,(\rho_k-\rho_0)\Delta+\tau_{k,c})\right|^2 + \frac{\rho_0^\beta}{E_s/N_0}\right)} \quad (10)$$

ponentially distributed RV having a unit average[1]. Therefore, since the denominator of SINR is non-negative, we obtain (10) when we condition on the set of RVs $\left\{\alpha_k, \rho_k, b_{k,n}^-, b_{k,n}^+ \forall k,n\right\}$

Let the value of $\mathcal{W}_m(z)$ be shown in (11), where the expectation is taken over the RVs $\left\{\alpha_k, \rho_k, b_{k,n}^-, b_{k,n}^+ \forall n,k\right\}$. Then, we have for the CDF

$$\Pr(\mathrm{SINR}\le z) = 1 - \mathcal{W}_m(z)\, e^{-z\frac{\rho_0^\beta}{E_s/N_0}}. \quad (12)$$

Now, since the RVs $\{\rho_k, \alpha_k, k=1,2,\ldots,K\}$ are mutually independent, (11) reduces into the product shown in (13), where the value of $\mathcal{M}_k(z,\rho_k)$ is shown in (14).

In arriving at (13), we have used the assumptions that α_k are Bernoulli RVs with $\Pr\{\alpha_k = 1\} = q$, and that the K interfering transmitters are independent and uniformly distributed in a circle of radius D around the reference receiver. (Note that when a point is uniformly distributed in a circle of unit radius then $\Pr(\rho_k < x) = \frac{\pi x^2}{\pi}$, $x<1$. Therefore, the pdf of ρ_k is $f_{\rho_k}(x) = 2x$ when $x\le 1$, and $f_{\rho_k}(x) = 0$ when $x>1$.)

The computations of $\mathcal{M}_k(z,\rho_k)$ in the case of arbitrary subcarrier assignment schemes may involve averaging over a large set of discrete RVs $\left\{b_{k,n}^-, b_{k,n}^+, n\in\mathcal{A}_k\right\}$, which could be very cumbersome when $|\mathcal{A}_k| >> 1$. However, exact simple expressions can be derived in the special case of interleaved subcarrier assignment schemes, as can be seen in the next subsection. On the other hand, in order to facilitate the computation of $\mathcal{M}_k(z,\rho_k)$ in the case of block-subcarrier assignment schemes, we present accurate approximations which are based on the conditional Gaussian approximations, and tight lower bounds which are based on the Jensen's inequality.

A. Exact Expressions of $\mathcal{M}_k(z,\rho_k)$ in case of Interleaved Subcarrier Assignments

For the sake of performance analysis, we assume here that all subcarriers in the vicinity of subcarrier m are allocated to different distinct users. This implies that at most one subcarrier from each set $\mathcal{A}_k$ may interfere with subcarrier m. Let the index of this subcarrier be denoted by a_k. Then (14) reduces into a simpler expression shown in (15), which involves averages with respect to two symbols only. Let $\mathcal{Q}(z) = \mathbb{E}\left[e^{-z\left|\left(b_{k,a_k}^- - b_{k,a_k}^+\right)\right|^2}\right]$, where the average is taken over the information symbols b_{k,a_k}^- and b_{k,a_k}^+. Then (15) can be expressed as shown in (16).

In the case of square M-QAM with Gray coding, $\mathrm{Re}b_{k,n}^+$ and $\mathrm{Im}b_{k,n}^+$ are selected independently over the set $\left\{\pm1, \pm3, ..., \pm\left(\sqrt{M}-1\right)\right\}$, and it can be verified that

$$\begin{aligned}\Pr\left\{\mathrm{Re}\left\{b_{k,n}^- - b_{k,n}^+\right\} = 2\mu\right\} &= Pr\left\{\mathrm{Im}\left\{b_{k,n}^- - b_{k,n}^+\right\} = 2\mu\right\} \\ &= \begin{cases}\frac{\sqrt{M}-\mu}{M}, & \mu = 0, \pm1, \pm2, \ldots, \pm\left(\sqrt{M}-1\right) \\ 0, & \text{otherwise.}\end{cases}\end{aligned}$$

Therefore

$$\begin{aligned}\mathcal{Q}(z) &= \mathbb{E}\left[e^{-z\left|\left(b_{k,n}^- - b_{k,n}^+\right)\right|^2}\right] \\ &= \mathbb{E}\left[e^{-z\left(\mathrm{Re}\left\{b_{k,n}^- - b_{k,n}^+\right\}\right)^2}\right]\mathbb{E}\left[e^{-z\left(\mathrm{Im}\left\{b_{k,n}^- - b_{k,n}^+\right\}\right)^2}\right] \\ &= \left[\frac{\sqrt{M}}{M} + 2\sum_{\mu=1}^{\sqrt{M}-1}\frac{\sqrt{M}-\mu}{M}e^{-4z\mu^2}\right]^2. \end{aligned} \quad (17)$$

B. Conditional Gaussian Approximation

Exact evaluation of $\mathcal{M}_k(z,\rho_k)$ in the case of block-subcarrier assignment schemes involves a large number of discrete RVs $\left\{b_{n,k}^-, b_{k,n}^+, \forall n\in\mathcal{A}_k\right\}$ for which exact averaging would require a large number of operations particularly in the case of high order modulations. In order to reduce the computational complexity required to compute (14) in the case of block-subcarrier assignment schemes, we propose a new improved Gaussian approximation method. Let

$$\vartheta_{k,c} = \sqrt{\gamma_c}\sum_{n\in\mathcal{A}_k}\left(b_{k,n}^- - b_{k,n}^+\right)\mathcal{G}\left(n-m, (\rho_k-\rho_0)\Delta+\tau_{k,c}\right). \quad (18)$$

Now, when ρ_k is given, then $\vartheta_{k,c}$ becomes a sum of "independent" RVs. However, the set of C RVs

[1]It can be seen that because of the assumption of independent paths and the normalization of the power delay profile, then $G_{0,m}$ becomes a zero-mean complex Gaussian variable with unit variance.

$$\mathcal{W}_m(z) = \mathbb{E}\left[e^{-z\sum_{k=1}^{K}\left(\frac{\rho_k}{\rho_0}\right)^{-\beta}\alpha_k \sum_{c=0}^{C-1}\gamma_c\left|\sum_{n\in\mathcal{A}_k}\left(b_{k,n}^{-}-b_{k,n}^{+}\right)\mathcal{G}(n-m,(\rho_k-\rho_0)\Delta+\tau_{k,c})\right|^2}\right] \tag{11}$$

$$\begin{aligned}\mathcal{W}_m(z) &= \prod_{k=1}^{K}\mathbb{E}\left[e^{-z\left(\alpha_k\left(\frac{\rho_k}{\rho_0}\right)^{-\beta}\sum_{c=0}^{C-1}\gamma_c\left|\sum_{n\in\mathcal{A}_k}\left(b_{k,n}^{-}-b_{k,n}^{+}\right)\mathcal{G}(n-m,(\rho_k-\rho_0)\Delta+\tau_{k,c})\right|^2\right)}\right] \\ &= \prod_{k=1}^{K}\left[1-q+q\int_0^1 \mathcal{M}_k(z,x)\,2xdx\right] \end{aligned} \tag{13}$$

$$\mathcal{M}_k(z,\rho_k) = \mathbb{E}\left[e^{-z\left(\frac{\rho_k}{\rho_0}\right)^{-\beta}\sum_{c=0}^{C-1}\gamma_c\left|\sum_{n\in\mathcal{A}_k}\left(b_{k,n}^{-}-b_{k,n}^{+}\right)\mathcal{G}(n-m,(\rho_k-\rho_0)\Delta+\tau_{k,c})\right|^2}|\rho_k\right] \tag{14}$$

$$\mathcal{M}_k(z,\rho_k) = \mathbb{E}\left[e^{-z\left(\frac{\rho_k}{\rho_0}\right)^{-\beta}\sum_{c=0}^{C-1}\gamma_c\left|\left(b_{k,a_k}^{-}-b_{k,a_k}^{+}\right)\right|^2|\mathcal{G}(a_k-m,(\rho_k-\rho_0)\Delta+\tau_{k,c})|^2}|\rho_k\right] \tag{15}$$

$$\mathcal{M}_k(z,\rho_k) = \mathcal{Q}\left(z\left(\frac{\rho_k}{\rho_0}\right)^{-\beta}\sum_{c=0}^{C-1}\gamma_c\left|\mathcal{G}(a_k-m,(\rho_k-\rho_0)\Delta+\tau_{k,c})\right|^2\right) \tag{16}$$

$\{\vartheta_{k,c}, c=0,1,\ldots C-1\}$ are not mutually independent (even when ρ_k is given). Therefore, we approximate the set of RVs $\{\vartheta_{k,c}, c=0,1,\ldots C-1\}$ by joint complex Gaussian RVs (conditioned on ρ_k) having zero means and (conditional) correlations given by

$$\begin{aligned}&\mathbb{E}\left[\vartheta_{k,j}\vartheta_{k,i}^{*}|\rho_k\right] \\ &= \tfrac{4}{3}(M-1)\sqrt{\gamma_j\gamma_i}\sum_{n\in\mathcal{A}_k}\mathcal{G}(n-m,(\rho_k-\rho_0)\Delta+\tau_{k,j}) \\ &\times\mathcal{G}^{*}(n-m,(\rho_k-\rho_0)\Delta+\tau_{k,i}), \qquad i,j=0,1,\ldots,L-1\end{aligned} \tag{19}$$

where we have used the fact that for a Gray coded square MQAM, $\mathbb{E}\left[\left|\left(b_{k,n}^{-}-b_{k,n}^{+}\right)\right|^2\right] = 2\mathbb{E}\left[\left|b_{k,n}^{-}\right|^2\right] = 4\mathbb{E}\left[\mathrm{Re}^2 b_{k,n}^{-}\right] = 4\frac{M-1}{3}$.

That is, the exponent of (14) is approximated by a sum of L Gaussian quadratic forms. Now, using known results for the moment generating functions of the complex Gaussian quadratic forms (e.g. [21]), we arrive at the following closed-form approximate expression for (14)

$$\begin{aligned}\mathcal{M}_k(z,\rho_k) &= \mathbb{E}\left[e^{-z\left(\frac{\rho_k}{\rho_0}\right)^{-\beta}\sum_{c=0}^{C-1}|\vartheta_{k,c}|^2}|\rho_k\right] \\ &\approx \frac{1}{\left|\boldsymbol{I}_C + z\left(\frac{\rho_k}{\rho_0}\right)^{-\beta}\boldsymbol{\Lambda}_k\right|}\end{aligned} \tag{20}$$

where $\boldsymbol{I}_C$ is the $C\times C$ identity matrix, and $\boldsymbol{\Lambda}_k$ is the correlation matrix (conditioned on ρ_k) of the jointly complex Gaussian vector $\{\vartheta_{k,0},\vartheta_{k,1},\ldots,\vartheta_{k,C-1}\}$ with elements defined in (19).

It is to be emphasized at this point that the proposed Gaussian approximation is distinctive from the classical Gaussian approximation methods which are commonly used in interference analysis in wireless systems[2].

C. A Lower Bound on $\mathcal{M}_k(z,\rho_k)$

A lower bound on $\mathcal{M}_k(z,\rho_k)$, which is valid for arbitrary subcarrier assignment schemes, is readily obtained by noticing that the function $\exp(-zx)$ is convex $\forall z, x>0$, and therefore Jensen's inequality can be invoked to show the result in (21).

Upper bounds on the exact bit and symbol error probabilities are then obtained when (21) is used in (13) instead of (14).

IV. Average Error Rate Analysis

With the distribution of SINR on hand, it is straightforward to derive exact expressions for average error rates. Though the probability density function of SINR is readily obtained by taking the derivative of (12), however, it is possible to compute the desired averages directly in terms of the CDF. For instance, by using the rules of the integration by parts, the average of an arbitrary function $g(\mathrm{SINR})$ can be computed as follows

$$\mathbb{E}\left[g(\mathrm{SINR})\right] = g(0) + \int_0^{\infty} g'(z)\Pr(\mathrm{SINR}>z)\,dz \tag{22}$$

where $g'(z)$ is the first derivative of $g(z)$.

1) Average SER: The conditional SER of square Gray-coded MQAM is [23, eq. (10.32)]

$$p_s(\mathrm{SINR}) = 1-\left(1-\left(1-\tfrac{1}{\sqrt{M}}\right)\mathrm{erfc}\sqrt{\mathrm{SINR}}\right)^2. \tag{23}$$

Therefore, the average SER is obtained from (22) and (23) to yield (24), where $E_b = E_s\frac{\frac{2}{3}(M-1)}{\log_2 M}$ is the "average" signal-to-noise ratio per bit (SNR).

[2]In classical Gaussian approximation methods, the (non-Gaussian) decision variable (e.g., η_m in (6)) is approximated by a single Gaussian RV. This is in order employ the readily known expressions of error rates in AWGN, and therefore simplify the evaluation of average error rates, which otherwise become non-trivial.

$$\begin{aligned}\mathcal{M}_k(z,\rho_k) &= \mathbb{E}\left[e^{-z\left(\frac{\rho_k}{\rho_0}\right)^{-\beta}\sum_{c=0}^{C-1}\gamma_c\left|\sum_{n\in\mathcal{A}_k}\left(b_{k,n}^{-}-b_{k,n}^{+}\right)\mathcal{G}(n-m,(\rho_k-\rho_0)\Delta+\tau_{k,c})\right|^2}|\rho_k\right]\\ &\geq e^{-z\left(\frac{\rho_k}{\rho_0}\right)^{-\beta}\sum_{c=0}^{C-1}\gamma_c\mathbb{E}\left[\left|\sum_{n\in\mathcal{A}_k}\left(b_{k,n}^{-}-b_{k,n}^{+}\right)\mathcal{G}(n-m,(\rho_k-\rho_0)\Delta+\tau_{k,c})\right|^2\right]}\\ &= e^{-z\mathbb{E}\left[\left|b_{k,n}^{-}-b_{k,n}^{+}\right|^2\right]\left(\frac{\rho_k}{\rho_0}\right)^{-\beta}\ \sum_{c=0}^{C-1}\gamma_c\sum_{n\in\mathcal{A}_k}\mathbb{E}\left[\left|b_{k,n}^{-}-b_{k,n}^{+}\right|^2\right]|\mathcal{G}(n-m,(\rho_k-\rho_0)\Delta+\tau_{k,c})|^2}\\ &= e^{-z\frac{4}{3}(M-1)\left(\frac{\rho_k}{\rho_0}\right)^{-\beta}\ \sum_{c=0}^{C-1}\gamma_c\sum_{n\in\mathcal{A}_k}|\mathcal{G}(n-m,(\rho_k-\rho_0)\Delta+\tau_{k,c})|^2}\end{aligned} \tag{21}$$

$$p_s=\frac{M-1}{M}-2\left(1-\frac{1}{\sqrt{M}}\right)\int_0^{\infty}\frac{1-\left(1-\frac{1}{\sqrt{M}}\right)\operatorname{erfc}\sqrt{z}}{\sqrt{\pi z}}e^{-z\left(1+\frac{2(M-1)}{3\log_2 M}\frac{N_0}{E_b}\right)}\mathcal{W}(z)\,dz \tag{24}$$

2) Average BER: General expressions for bit error probabilities of generalized square M-QAM are given in [22], which can be written in the following form

$$p_b(\text{SINR})=\sum_{\mu=0}^{\sqrt{M}-2}a_\mu\operatorname{erfc}\left((2\mu+1)\sqrt{\text{SINR}}\right) \tag{25}$$

where a_μ are some constants that depend on the constellation size M. For instance $a_0=\frac{1}{2}$ in case of QPSK, $a_\mu\in\left\{\frac{3}{8},\frac{2}{8},\frac{-1}{8}\right\},\mu=0,1,2$, in case of 16-QAM, whereas $a_\mu\in\left\{\frac{7}{24},\frac{6}{24},\frac{-1}{24},0,\frac{1}{24},0,\frac{-1}{24}\right\},\ \mu=0,1,\ldots 6$, in case of 64-QAM. Therefore

$$p_b=\frac{1}{2}-\int_0^{\infty}\frac{e^{-z}}{\sqrt{\pi z}}\sum_{\mu=0}^{\sqrt{M}-2}a_\mu e^{-\frac{z}{E_b/N_0}\frac{2(M-1)}{3(2\mu+1)^2\log_2 M}}\mathcal{W}\left(\frac{z}{(2\mu+1)^2}\right)dz. \tag{26}$$

In summary, (24) and (26) are, respectively, the new closed form expressions for the symbol and bit error rates of MQAM-OFDMA. Their accuracy depend on which expression for $\mathcal{M}_k(z,\rho_k)$ is used. Exact bit/symbol error rates are obtained when (16) is used, whereas approximations or upper bounds are obtained when (20) or (21) are used instead.

V. The Impact of Dynamic FFT Window Positioning

So far, we have been confined to the special case of static FFT windows, where all FFT windows are positioned specifically at (T_g,T_g+T). This is a quite common assumption in the literature of OFDM where the CPs are used primarily to provide multipath immunity. Although, this will also alleviate some of the MUI caused by late arriving subcarriers, it will not provide immunity against the early arriving subcarriers, and the performance of OFDMA deteriorates substantially even when the CP length exceeds the maximum misalignment time (as will be seen in next section). Therefore, in order to completely alleviate the MUI, it is necessary to adequately adjust the position of the FFT window within the OFDMA symbol so that all OFDMA signals appear orthogonal at the receiver, Fig. 1. Notice that, by extending the CP length, the samples required for performing the FFT at the receiver can be taken anywhere over the OFDMA symbol time-interval (but not earlier than $\tau_{\max}$, the maximum delay spread of the multipath channel).

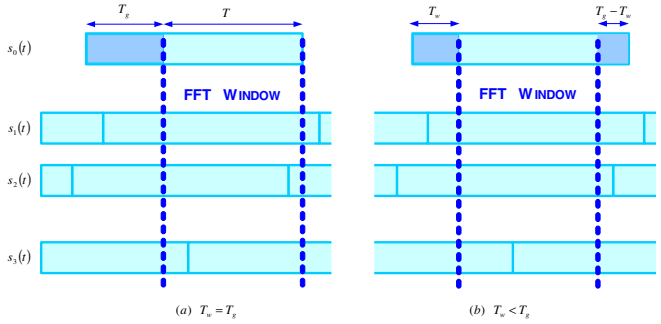

Fig. 1. Impact of FFT window positioning.

It can be seen that when $\Delta<1$ and the CP duration is extended beyond the maximum propagation delay, $T_g\geq\Delta+\tau_{\max}$, then the MUI can be completely alleviated by allowing each receiver to dynamically position its own FFT window at $T_w=(1-\rho_0)\Delta+\tau_{\max}$.

It is worth mentioning that extending the duration of the FFT window beyond what is required to alleviate the inter-symbol interference is a known simple technique for mitigating the MUI resulting from timing misalignments in uplink OFDMA [6]. On the other hand, the concept of dynamically positioning the FFT window has been used in single frequency networks [20].

The analysis presented in the previous sections can be extended straightforwardly to include OFDMA having arbitrary FFT window positions. Let the FFT window be taken over the time interval (T_w,T_w+T), where $\tau_{\max}<T_w\leq T_g$, Fig. 1. Then, it can be seen that the CDF of SINR is still given by (12) (together with (13) and (14)) but with $\mathcal{G}_0(p,y)$, in (7), being replaced with the general expression shown in (27), which depends on the FFT window position T_w where $N_w=\frac{T_w}{T_s}$ (which is assumed integer).

VI. The Spectral Efficiency

Though CPs have a positive effect on counteracting the MUI due to time-misalignments, extending their length beyond the maximum delay spread of the channel might lead to a substantial decrease in the spectral efficiency. Therefore, it is of both theoretical and practical interests to give insight into the penalty of the time-misalignments and the effectiveness of the CPs on the overall spectral efficiency of the OFDMA ad hoc network. In this regard, cutoff rates are commonly used to

$$\mathcal{G}_0(p,y,T_w)=\begin{cases}0, & 0<y\bmod(T+T_g)\le T_w\\ \dfrac{\sin\left(\pi\dfrac{\left\lfloor\frac{y\bmod(T+T_g)}{T_s}\right\rfloor-N_w}{N}p\right)}{N\sin\left(\frac{\pi}{N}p\right)}e^{j\frac{\pi p}{N}\left(\left\lfloor\frac{y\bmod(T+T_g)}{T_s}\right\rfloor+N_w-1\right)}, & T_w<y\bmod(T+T_g)\le T_w+T\\ 0, & T_w+T<y\bmod(T+T_g)\le T_g+T.\end{cases} \tag{27}$$

measure the spectral efficiency of different digital modulation schemes in terms of information bits/symbol/Hz.

The cutoff rate $\mathcal{R}_0$ of a coded modulation system is a measure of the number of information bits that can be transmitted per symbol time with arbitrarily small probability of error when a finite complexity coding scheme is used. Under the usual assumption of ideal symbol interleaving and uniform input distribution, the cutoff rate in the Gaussian additive channel is [23, pp. 773] $\mathcal{R}_0=-\log_2\left(\bar{\mathcal{D}}\right)$, where $\bar{\mathcal{D}}=\mathbb{E}\left[\mathcal{D}\left(\text{SINR}\right)\right]$, and

$$\mathcal{D}\left(\text{SINR}\right)=\left[\frac{1}{\sqrt{M}}\sum_{\mu=0}^{\sqrt{M}-1}\sum_{\mu'=0}^{\sqrt{M}-1}e^{-\left|b_\mu-b_{\mu'}\right|^2\frac{\text{SINR}}{4}}\right]^2 \tag{28}$$

which we can rewrite as

$$\mathcal{D}\left(\text{SINR}\right)=\left(\frac{1}{\sqrt{M}}+2\sum_{\mu=1}^{\sqrt{M}-1}\frac{\sqrt{M}-\mu}{M}e^{-\mu^2\text{SINR}}\right)^2. \tag{29}$$

Assuming that the receiver treats the MUI as the AWGN, the cutoff rate is obtained by calculating the average of (29) with respect to SINR. It can be shown by using (12) that

$$\bar{\mathcal{D}}=1-4\int_0^\infty\left(\frac{1}{\sqrt{M}}+2\sum_{\mu=1}^{\sqrt{M}-1}\frac{\sqrt{M}-\mu}{M}e^{-\mu^2z}\right)\times\left(\sum_{\mu=1}^{\sqrt{M}-1}\mu^2\frac{\sqrt{M}-\mu}{M}e^{-\mu^2z}\right)e^{-\frac{z}{E_b/N_0}\frac{2(M-1)}{3\log_2 M}}\mathcal{W}(z)\,dz. \tag{30}$$

VII. Numerical Examples

In this section, we present some numerical and simulation results. For the sake of numerical examples, we consider a 50% loaded system with $q=0.5$ in a multipath Rayleigh fading channel with exponential power-delay profile, where $\gamma_c=\gamma_0e^{-c/4}$, $c=1,2,\ldots,C-1$, and $C=10$. $\tau_{k,c}=\frac{c}{C-1}\tau_{\max}\ \forall k$, where the maximum delay spread is set at $\tau_{\max}=\frac{T}{10}$, and the path-loss exponent $\beta=4$. The total number of subcarriers is fixed at $N=1024$, and the number of subcarriers in a block in the case of block-subcarrier assignment scheme is 10.

Firstly, the accuracy of the new exact and approximate expressions of BER is investigated in Figs. 2 and 3 for interleaved and blocked subcarrier assignment schemes, respectively. Here the average BER of QPSK is plotted against the normalized range of the useful signal ρ_0, when $T_w=T_g=2\tau_{\max}$, and for three different values of the normalized maximum propagation delay $\Delta\in\{0.01,01,1\}$. Both theoretical and simulation results are displayed in Figs. 2

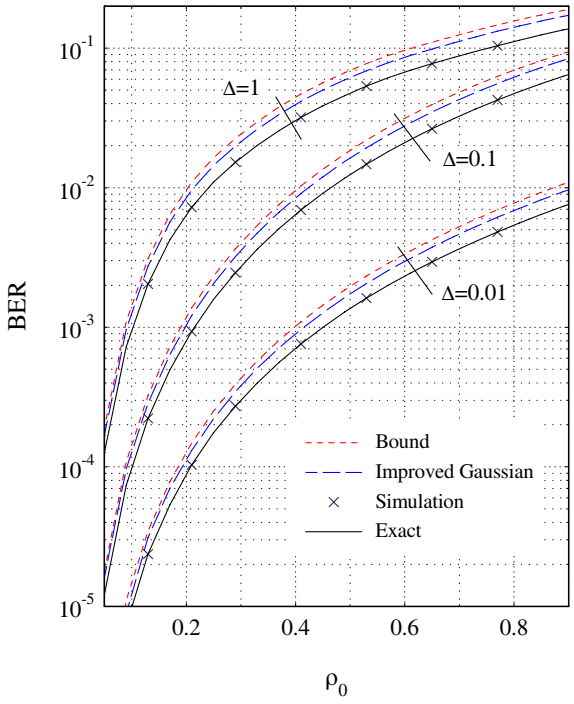

Fig. 2. Theoretical and simulation results for the average BER of QPSK against the range of the useful signal (ρ_0) in the case of interleaved-subcarrier assignment scheme. $T_w=T_g=0.2T$, and $\Delta\in\{0.01,0.1,1\}$.

and 3. The theoretical results are evaluated by using (26), but with three different expressions of $\mathcal{M}_k(z,\rho_k)$ which are given in (16), (20) and (21), for the exact, improved Gaussian approximation, and the bound, respectively. The exact theoretical results are shown in Fig. 2 for interleaved subcarrier assignment scheme, which show excellent match to the relevant simulation results. On the other hand, as far as the accuracy of the proposed approximations and bounds is concerned, one can see from Figs. 2 and 3, that the difference between the approximate and exact (or simulation) results is diminished even in the case of the interleaved subcarrier assignments where $|\mathcal{A}_k|=1\forall k$. More interestingly, Figs 2 and 3 reveal that the proposed upper bound on BER is in fact a tight upper bound, and therefore can be employed to provide an efficient and accurate method for performance evaluation of OFDMA with arbitrary subcarrier assignments.

In Fig. 4, we consider an OFDMA system without extended CPs, and investigate the impact of the maximum propagation delay on the cutoff rate. Here, we fix the CP time-interval at $T_g=\tau_{\max}$, and plot the cutoff rate against the normalized maximum propagation delay (Δ) for both interleaved and block subcarrier assignment schemes, and for several modulation orders. We observe a dramatic loss in the cutoff rate

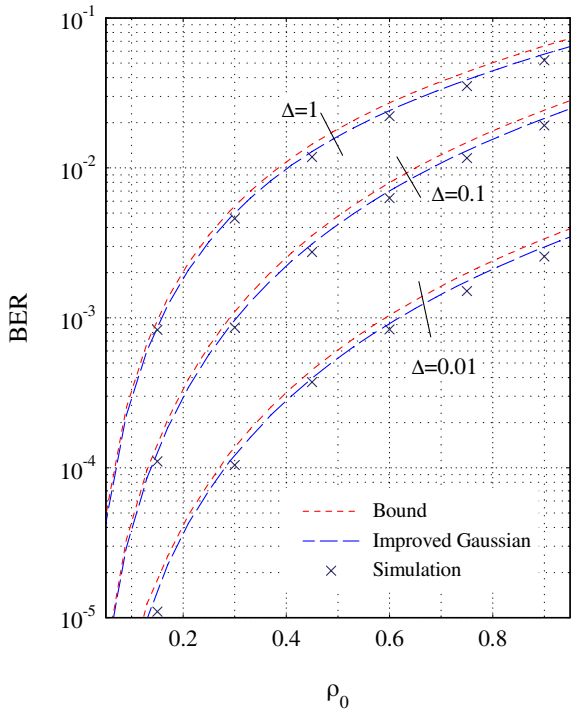

Fig. 3. Theoretical and simulation results for the average BER of QPSK against the range of the useful signal (ρ_0) in the case of block-subcarrier assignment scheme. $T_w = T_g = 0.2T$, and $\Delta \in \{0.01, 0.1, 1\}$.

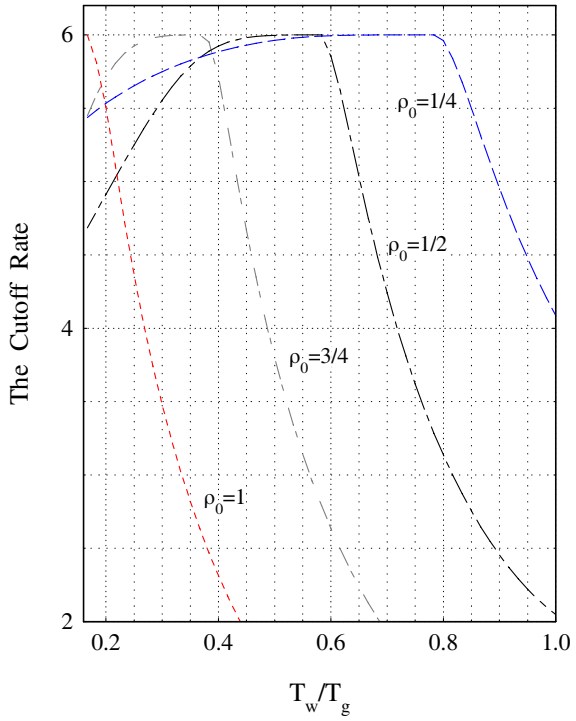

Fig. 5. The cutoff rate against the relative FFT window position, T_w/T_g, in case of 64QAM with interleaved subcarrier assignment scheme. $T_g = 0.6T$, $\Delta = T/2$, and $\rho_0 \in \{\frac{1}{4}, \frac{1}{2}, \frac{3}{4}, 1\}$.

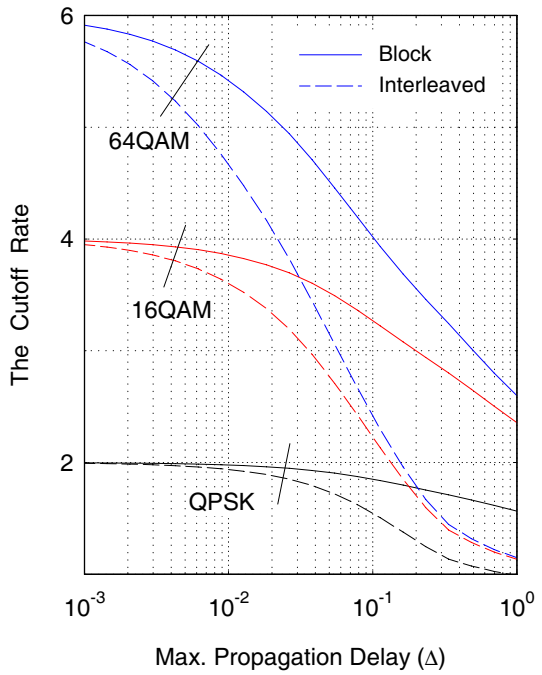

Fig. 4. The cutoff rate of BPSK, QPSK, 16QAM and 64QAM against the normalized maximum propagation delay in the case of interleaved-subcarrier assignment. $\rho_0 = \frac{2}{3}$, $T_g = \tau_{\max} = T/10$.

with increasing the maximum propagation delay, particularly at higher levels of modulation. The reason why QPSK is less sensitive to timing misalignment than 64QAM can be explained in view of (8) by observing that the MUI from an arbitrary subcarrier n occurs only whenever $b_{k,n}^- \neq b_{k,n}^+$ regardless of the level of the time misalignment. Hence, MUI may occur with probability $\Pr\left\{b_{k,n}^- \neq b_{k,n}^+\right\} = \frac{63}{64} \approx 1$ in the case of 64QAM, whereas this probability drops to only $\frac{1}{4}$ in the case of QPSK. Fig. 4 also reveals that the block subcarrier assignment scheme outperforms its counterpart. This behavior can be explained in the view of the fact that no MUI may occur from the subcarriers in $\mathcal{A}_0$ (a consequence of the assumption that the reference receiver is perfectly synchronized to the desired transmitter). That is, if the reference subcarrier m is at the lower edge of the block in a block subcarrier assignment scheme, then MUI might be generated only from the lower subcarriers $\{\ldots, m-2, m-1\}$, but not from $\{m+1, m+2, \ldots\}$. On the other hand, a subcarrier m in the interleaved scheme is subjected to MUI from all adjacent subcarriers $\{\ldots, m-2, m-1, m+1, m+2, \ldots\}$.

Fig. 5 demonstrates the benefits of dynamic FFT window positioning on the performance of OFDMA. Here, the cutoff rate of 64QAM with interleaved subcarrier assignment scheme is plotted against the normalized FFT window position for several values of $\rho_0 \in \{\frac{1}{4}, \frac{1}{2}, \frac{3}{4}, 1\}$ in a network having a maximum propagation delay of $\Delta = T/2$. The total length of the CP is fixed at $T_g = 0.6T$. As expected, the cutoff rate is maximized when the FFT window is positioned specifically at $T_w = (1-\rho_0)\Delta + \tau_{\max}$. For instance, it can be verified that the maximum cutoff rate at $\rho_0 = \frac{1}{2}$ is achieved when $T_w = 0.583T_g = 0.35T$. We also observe from Fig. 5 that the shape of the cutoff rates becomes flatter at lower values of ρ_0. This implies that the performance of the OFDMA systems becomes less sensitive to the optimum window position when the distance between the reference receiver and the desired transmitter becomes shorter. This is because the early arriving interfering subcarriers are more harmful than the later arrivals.

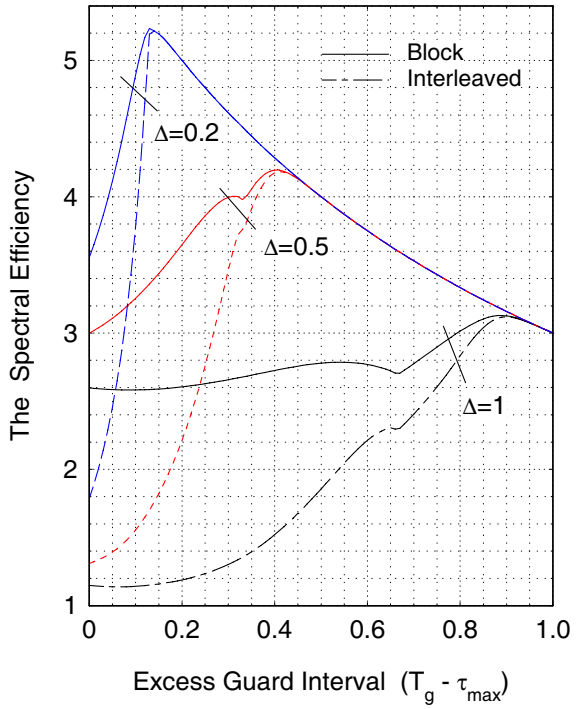

Fig. 6. The normalized cutoff rate $\frac{T}{T+T_g-\tau_{\max}}R_0$ of 64QAM against the excess guard interval, in the case of interleaved subcarrier assignment. $\rho_0 = 2/3$, and $\Delta \in \{0.2, 0.5, 0.7, 1\}$.

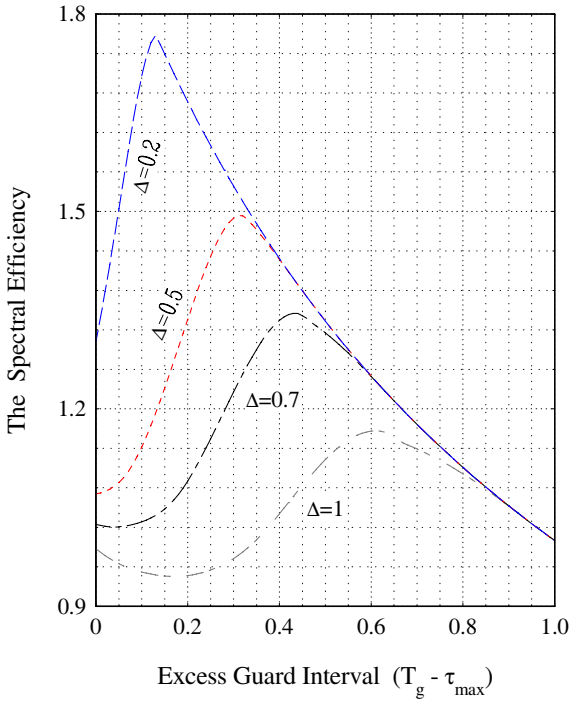

Fig. 7. The normalized cutoff rate $\frac{T}{T+T_g-\tau_{\max}}R_0$ against the excess guard interval for QPSK with interleaved subcarrier assignment. $\rho_0 = 2/3$, and $\Delta \in \{0.2, 0.5, 0.7, 1\}$.

That is, when the reference signal is located at the edge $\rho_0 = 1$, then all other transmitters are located in $\rho_k \in (0, 1)$, which are stronger than the useful signal, and therefore will bring on a significant amount of MUI. On the other hand, when the desired user is located at $\rho_0 = \frac{1}{4}$, then on the average $\frac{15}{16}$ of other transmitters will be located in $\rho_k \in \left(\frac{1}{4}, 1\right)$, which are weaker than the useful signal, and therefore produce weaker MUI. This suggests that when the total guard-interval T_g is less than the maximum propagation delay, then the best performance is obtained when each user allocates its own FFT window at $T_w = \max\{\tau_{\max}, T_g - \rho_0\Delta\}$.

In Figs. 6-8, we study the net effect of guard time intervals on the overall spectral efficiency of OFDMA. Notice that, though extending the CP length has the desired effect of combating MUI, however, CPs contribute to the overheads that reduce the net information transmission rates. In this paper we propose to measure the overall spectral efficiency of OFDMA systems in terms of the normalized cutoff rate $\frac{T}{T+T_g-\tau_{\max}}R_0$. In Figs. 6-8 we plot the spectral efficiency against the excess length of the guard-interval $T_g - \tau_{\max}$ for several values of maximum propagation delays.

Normalized cutoff rates of 64QAM is given in Fig. 6 for both block and interleaved subcarrier assignment schemes. It is observed that in this case, and for both interleaved and block subcarrier assignment schemes, the optimum choice of CP length equals $T_g \approx \Delta$. Notice that the MUI is alleviated completely when $T_g = \tau_{\max} + \Delta$. This implies that at higher modulation levels, the penalty of lengthening the guard-interval is compensated by the improvement in the cutoff rates. Though both interleaved and block assignment schemes have the same optimum performance, however, Fig. 6 reaffirms that the block schemes is less sensitive to the timing misalignments.

The spectral efficiency of QPSK are given in Figs. 7-8 for both interleaved and block subcarrier assignment schemes, respectively. We observe from Fig. 8 for the block subcarrier schemes that excess guard-intervals are not required in the case of low order modulations such as QPSK. This is in contrast to the interleaved subcarrier schemes shown in Fig. 7, where excess guard-intervals are required to maximize the spectral efficiency. However, comparing Fig. 7 with Fig. 6 for 64QAM, we see that the optimum lengths of the guard-intervals in QPSK are shorter than the relevant lengths in 64QAM. For instance when $\Delta = 1$, then the optimum length is $T_g \approx 0.7$ (instead of 1 in case of 64QAM).

Figs. 5-8 confirm that the spectral efficiency can be maximized by the adequate selection of the lengths of the guard-intervals and dynamic positioning of the FFT windows. Furthermore, the optimum guard-interval length depends on the subcarrier assignment scheme, modulation order, the operating SNR, and the maximum propagation delay.

VIII. Summary and Conclusions

We have presented a new precise theoretical performance analysis of the PHY layer of OFDMA ad hoc networks in the presence of MUI caused by time-misalignments, white Gaussian noise, and multipath Rayleigh fading. New exact expressions, and accurate approximations and bounds were derived for symbol and bit error rates of MQAM-OFDMA with arbitrary subcarrier assignment schemes. Cutoff rates were found and used to quantify the effectiveness of a common MUI mitigating technique, which is based on the extension of the

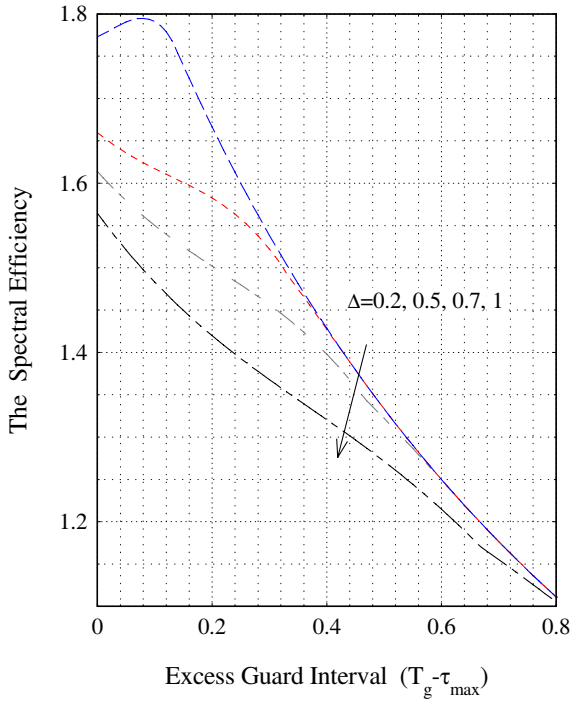

Fig. 8. The normalized cutoff rate $\frac{T}{T+T_g-\tau_{\max}}R_0$ against the excess guard interval for QPSK with block subcarrier assignment. $\rho_0 = 2/3$, and $\Delta \in \{0.2, 0.5, 0.7, 1\}$.

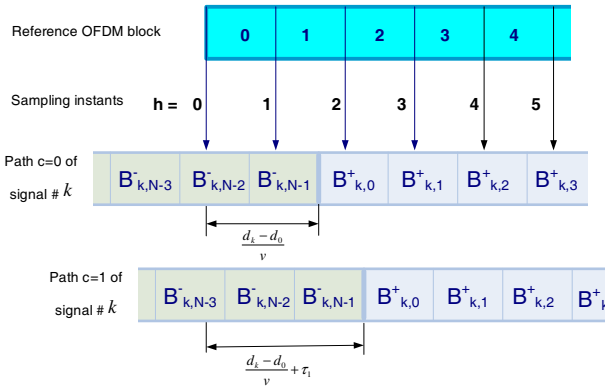

Fig. 9. Asynchronous interference. Two consecutive OFDM blocks from each path of signal k overlap with the reference OFDM block.

CP lengths beyond what is required to combat the multipath fading. The numerical results have shown that the spectral efficiency can be maximized by adequate guard-intervals and dynamic positioning of the FFT windows. Furthermore, the optimum length of the guard-interval depends on the subcarrier assignment scheme, the modulation order, the operating SNR, and the maximum propagation delay.

APPENDIX A

Note, from Fig. 9, that exactly two consecutive OFDM blocks from each interfering signal can occupy the time interval $\left(\frac{d_0}{v}, \frac{d_0}{v}+T+T_g\right)$. Let $x = \left\lfloor \frac{\left(\frac{d_k-d_0}{v}+\tau_{k,c}\right) \bmod (T_g+T)}{T_s} \right\rfloor$ be the delay index. Then

$$\chi_{t,k,c} = \begin{cases} B^-_{k,n}, & t = 0, 1, \ldots, x-1 \\ B^+_{k,n}, & t = x, x+1, \ldots N+N_g-1. \end{cases}$$

Therefore, the term in the brackets of the second line of (6) becomes when $x \leq N_g$

$$\frac{1}{\sqrt{N}} \sum_{t=N_g}^{N+N_g-1} \chi_{t,k,c} e^{-j2\pi \frac{tm}{N}} = \frac{1}{\sqrt{N}} \sum_{t=N_g}^{N+N_g-1} B^+_{k,n} e^{-j2\pi \frac{tm}{N}} = 0. \tag{31}$$

On the other hand, when $x > N_g$ we have the equation at the top of the next page.

But the term $\sum_{t=N_g}^{N+N_g-1} e^{j\frac{2\pi(n-m)t}{N}} = 0 \ \forall n \neq m$. Therefore, the last line reduces into

$$\begin{aligned} &\frac{1}{\sqrt{N}} \sum_{t=N_g}^{N+N_g-1} \chi_{t,k,c} e^{-j2\pi \frac{tm}{N}} \\ &= \sum_{n \in \mathcal{A}_k} \left(b^-_{k,n} - b^+_{k,n}\right) \frac{1}{N} \sum_{t=N_g}^{x-1} e^{j\frac{2\pi(n-m)t}{N}} \\ &= \sum_{n \in \mathcal{A}_k} \left(b^-_{k,n} - b^+_{k,n}\right) \frac{\sin\left(\frac{\pi}{N}(n-m)(x-N_g)\right)}{N \sin\left(\pi \frac{1}{N}(n-m)\right)} e^{j\frac{\pi(n-m)}{N}(x+N_g-1)}. \end{aligned} \tag{32}$$

REFERENCES

[1] L. Hanzo, M. Munster, B. J. Choi, and T. Keller, *OFDM and MC-CDMA for Broadband Multi-User Communications, WLANs, and Broadcasting*. Chichester, UK: IEEE Press - John Wiley, 2003.
[2] H. Liu and G. Li, *OFDM-Based Broadband Wireless Networks*. Hoboken, NJ: Wiley-Interscience, 2005.
[3] Y. Gao, H. Tian, L. Sun, and H. Xu, "Research on the access network and MAC technique for beyond 3G systems," *IEEE Personal Commun.*, vol. 14, pp. 57-61, Apr. 2007.
[4] IEEE Standard for Air Interface for Fixed Broadband Wireless Access Systems, IEEE 802.16, 2004.
[5] European Standard for Digital Video Broadcasting. Interaction Channel for Digital Terrestrial Television Incorporating Multiple Access OFDM, ETSI EN 301 958 V1.1.1, 2002.
[6] M. Morelli, C. Kuo, and M. Pun, "Synchronization techniques for orthogonal frequency division multiple access (OFDMA): a tutorial review," *Proc. IEEE*, vol. 95, pp. 1394-1427, July 2007.
[7] G. Kulkarni and M. Srivastava, "Subcarrier and bit allocation strategies for OFDMA based wireless ad hoc networks," in *Proc. IEEE GLOBECOM '02*, Nov. 2002, pp. 92-96.
[8] B. Gui, L. Dai, and L. J. Cimini, "Routing strategies in broadband multihop cooperative networks," in *Proc. IEEE Conf. Inform. Sci. Syst.*, Mar. 2007, pp. 661-666.
[9] T. Taiwen *et al.*, "Multichannel feedback in OFDM ad hoc networks," in *Proc. IEEE Conf. Sensor and Ad Hoc Commun. Networks*, Sep. 2006, pp. 701-704.
[10] Q. Xiangping and R. Berry, "Distributed power allocation and scheduling for parallel channel wireless networks," in *Proc. IEEE Conf. Modeling and Optimization Mobile, Ad Hoc, and Wireless Networks*, Apr. 2005, pp. 77-85.
[11] Y. Mostofi and D. C. Cox, "Mathematical analysis of the impact of timing synchronization errors on the performance of an OFDM systems," *IEEE Trans. Commun.*, vol. 54, pp. 226-230, Feb. 2006.
[12] J. Armstrong, "Analysis of new and existing methods of reducing intercarrier interference due to carrier frequency offset in OFDM," *IEEE Trans. Commun.*, vol. 47, pp. 365-369, Mar. 1999.
[13] K. Sathanathan and C. Tellambura, "Probability of error calculation of OFDM systems with frequency offset," *IEEE Trans. Commun.*, vol. 49, pp. 1884-1888, Nov. 2001.
[14] A. M. Tonello, N. Laurenti, and S. Pupolin, "Analysis of the uplink of an asynchronous multi-user DMT OFDMA system impaired by time offsets, frequency offsets, and multi-path fading," in *Proc. IEEE VTC'00-Fall*, Oct. 2000, pp. 1094–1099.

$$\frac{1}{\sqrt{N}}\sum_{t=N_g}^{N+N_g-1}\chi_{t,k,c}e^{-j2\pi\frac{tm}{N}} = \frac{1}{\sqrt{N}}\sum_{t=N_g}^{x-1}B_{k,n}^{-}e^{-j2\pi\frac{tm}{N}} + \frac{1}{\sqrt{N}}\sum_{t=x}^{N+N_g-1}B_{k,n}^{+}e^{-j2\pi\frac{tm}{N}}$$

$$= \frac{1}{N}\sum_{t=N_g}^{x-1}\sum_{n\in\mathcal{A}_k}b_{k,n}^{-}e^{j\frac{2\pi nt}{N}}e^{-j2\pi\frac{tm}{N}} + \frac{1}{N}\sum_{t=x}^{N+N_g-1}\sum_{n\in\mathcal{A}_k}b_{k,n}^{+}e^{j\frac{2\pi nt}{N}}e^{-j2\pi\frac{tm}{N}}$$

$$= \frac{1}{N}\sum_{n\in\mathcal{A}_k}\left\{b_{k,n}^{-}\sum_{t=N_g}^{x-1}e^{j\frac{2\pi(n-m)t}{N}} + b_{k,n}^{+}\left(\sum_{t=N_g}^{N+N_g-1}e^{j\frac{2\pi(n-m)t}{N}} - \sum_{t=N_g}^{x-1}e^{j\frac{2\pi(n-m)t}{N}}\right)\right\}$$

[15] M. El-Tanany, Y. Wu, and L. Hazy, "OFDM uplink for interactive broadband wireless: analysis and simulation in the presence of carrier, clock and timing errors," *IEEE Trans. Broadcast.*, vol. 47, pp. 3-19, Mar. 2001.

[16] M. Park, K. Ko, H. Yoo, and D. Hong, "Performance analysis of OFDMA uplink systems with symbol timing misalignment," *IEEE Commun. Lett.*, vol. 7, pp. 376-378, Aug. 2003.

[17] J. J. Yang and H. Haas, "Outage probability for uplink of cellular OFDM-FDMA system," in *Proc. IEEE VTC'04-Spring*, May 2004, pp. 2072-2076.

[18] Y.-H. You, W.-G. Jeon, J.-W. Wee, S.-T. Kim, I. Hwang, and H.-K. Song, "OFDMA uplink performance for interactive wireless broadcasting," *IEEE Trans. Broadcast.*, vol. 51, pp. 383-388, Sep. 2005.

[19] K. Raghunath and A. Chockalingam, "Sir analysis and interference cancellation in uplink OFDMA with large carrier frequency and timing offsets," in *Proc. IEEE WCNC'07*, Mar. 2007, pp. 997-1002.

[20] R. Brugger and D. Hemingway, "OFDM receivers: impact on coverage of inter-symbol interference and FFT window positioning," *EBU Technical Review*, July 2003.

[21] A. M. Mathai and S. B. Provost, *Quadratic Forms in Random Variables*. New York: Marcel Dekker, 1992.

[22] K. Cho and D. Yoon, "On the general BER expression of one- and two-dimensional amplitude modulations," *IEEE Trans. Commun.*, vol. 50, pp. 1074-1080, July 2002.

[23] M. Simon, S. Hinedi, and W. Lindsey, *Digital Communication Techniques: Signal Design and Detection*. Englewood Cliffs, NJ: Prentice-Hall, 1995.

Khairi Ashour Hamdi (M'99-SM'02) received the B.Sc. degree in electrical engineering from the Alfateh University, Tripoli, Libya, in 1981. He then received the M.Sc. degree (with Distinction) from the Technical University of Budapest, Budapest, Hungary, in 1988, and the Ph.D. degree in telecommunication engineering in 1993, awarded by the Hungarian Academy of Sciences. His current research interests include coexistence and interference analysis in unlicensed frequency bands and cognitive radio networks. He is now with the School of EEE, University of Manchester, Manchester U.K. Previously he was with the Department of ESE, University of Essex, Colchester, U.K. Dr. Hamdi was a BT research fellow during 2002, and was a visiting professor at Stanford University, USA, during 2008.